# Hijacking of the enterobactin pathway by a synthetic catechol vector designed for oxazolidinone antibiotic delivery in Pseudomonas aeruginosa

Lucile Moynié, Françoise Hoegy, Stefan Milenkovic, Mathilde Munier, Aurélie Paulen, Véronique Gasser, Aline Faucon, Nicolas Zill, James Naismith, Matteo Ceccarelli, et al.

# Hijacking of the enterobactin pathway by a synthetic catechol vector designed for oxazolidinone antibiotic delivery in *Pseudomonas aeruginosa*

Lucile Moynié,[1,2,] Françoise Hoegy,[3,4] Stefan Milenkovic,[5] Mathilde Munier, [3,4] Aurélie Paulen,[3,4] Véronique Gasser,[3,4] Aline L. Faucon,[3,4] Nicolas Zill,[3,4] James H Naismith,[1,2] Matteo Ceccarelli,[5,6] Isabelle J. Schalk, [3,4] Gaëtan L.A. Mislin*[,3,4]

[1] The Rosalind Franklin Institute, Harwell Campus, Oxfordshire, UK OX11 0QS

[2] Division of Structural Biology, Wellcome Trust Centre of Human Genomics, 7 Roosevelt Drive, Oxford, OX3 7BN

[3] CNRS, UMR7242 Biotechnologie et Signalisation Cellulaire, 300 Boulevard Sébastien Brant, F-67412 Illkirch, Strasbourg, France

[4] Université de Strasbourg, Institut de Recherche de l'Ecole de Biotechnologie de Strasbourg (IREBS), 300 Boulevard Sébastien Brant, F-67412 Illkirch, Strasbourg, France

[5] Department of Physics, University of Cagliari, 09042 Monserrato, Italy

[7] IOM/CNR, Sezione di Cagliari, University of Cagliari, 09042 Monserrato, Italy.

ORCID LM 0000-0002-4097-4331
JHN 0000-0001-6744-5061
GM 0000-0002-5646-3392
IS 0000-0002-8351-1679
MC 0000-0003-4272-902X
SM 0000-0002-1327-3564
FH 0000-0002-5440-5818
ALF 0000-0002-7057-0485
VG 0000-0002-0081-8000

*Keywords :* *Enterobactin, siderophore, linezolid, oxazolidinone, Trojan horse strategy, iron uptake, Pseudomonas aeruginosa, molecular simulations*

# ABSTRACT

Enterobactin is a tris-catechol siderophore used to acquire iron by multiple bacterial species. These enterobactin-dependent iron uptake systems have often been considered as a potential gate in the bacterial envelope through which one can shuttle antibiotics (Trojan horse strategy). In practice siderophore analogues containing catechol moieties have shown promise as vectors to which antibiotics may be attached. Bis- and Tris-Catechol Vectors (BCV and TCV respectively), were shown using structural biology and molecular modeling, to mimic enterobactin binding to the outer membrane transporter PfeA in *Pseudomonas aeruginosa.* TCV but not BCV, appears to cross the outer membrane via PfeA when linked to an antibiotic (linezolid). TCV is therefore a promising vector for Trojan horse strategies against *P. aeruginosa* confirming the enterobactin-dependent iron uptake system as a gate to transport antibiotics into *P. aeruginosa* cells.

# INTRODUCTION

Pathogenic bacteria remain a potent threat to humans despite the discovery of antibiotics which had appeared to promise the end of bacteria as the cause of human diseases. This is because the accumulated use and misuse of antibiotics has led to the evolution of antibiotic-resistant bacterial strains. Continuing development of new antibiotic compounds and antibacterial strategies is crucial to avoid a return to the pre-antibiotic world, there is particular concern over Gram-negative bacteria due to the paucity of new approaches. *Pseudomonas aeruginosa* is an opportunistic Gram-negative bacterium responsible of severe pulmonary infections affecting patients with cystic fibrosis and chronic obstructive pulmonary diseases (COPD).[1,2] This pathogen is also common in infections of severe burns and often occurs in clinical HIV and other immunocompromised patients.[3,4] *P. aeruginosa* is naturally resistant to many classes of antibiotics due to the low permeability of the outer membrane.[5] The outer membrane in Gram-negative bacteria in general is a selective barrier that restricts the penetration of many xenobiotic compounds not just antibiotics. The nutrient uptake systems act as selective openings in the bacterial envelope and have long been thought as a possible route for antibiotic uptake. This so called Trojan horse strategy should ideally utilize an essential and metabolically unsubstitutable nutrient to have a significant impact on the bacterial proliferation. Iron is the best nutrient that meet these criteria.

The concentration of free Fe(III) in normal human fluids is estimated around $10^{-24}$ M reflecting the inherent lack of bioavailability of the element. This presents a challenge for pathogenic bacteria where an Fe(III) concentration in the micromolar range was estimated to be optimal for bacterial proliferation.[6,7] To surmount this challenge bacteria have evolved efficient uptake systems able to give them access to iron from their environment.[8] One example is the ubiquitous siderophore-dependent iron transport systems. Siderophores are small Fe(III) chelating secondary metabolites secreted by bacteria, with diverse chemical structures and metal-to-

ligand stoichiometries.[9,10] The ferric complexes are next recognized by specific bacterial outer membrane transporters and imported back into the bacteria.[11,12] The energy necessary for this active uptake through the outer membrane is provided by the inner membrane TonB machinery and proton-motive force.[11-14] Some siderophores release iron in the bacterial periplasm whilst other siderophores cross the inner membrane before delivering the iron. In both scenarios, iron release from siderophores involves a reductive process sometimes coupled to a chemical modification or hydrolysis of the siderophore.[15,16]

Conjugates between siderophores and antibiotics were shown to hijack these uptake systems, leading to the accumulation of the drug in the bacterial inner compartments.[17] In many cases these sideromycins behave like Trojan horses and have a significantly higher antibacterial activity compared to the unconjugated drug.[17-31] Catechol siderophores are attractive vectors because of their (1) high affinity for iron(III), (2) occurrence in multiple bacterial species and strains,[9] (3) versatile chemical synthesis.[18,23,32,33] The archetypal catechol siderophore enterobactin (ENT) **1** is a cyclic trimer of 2,3-dihydroxybenzyl-serine (DHBS) used by many pathogenic bacteria,[34] even those that do not produce the metabolite (iron piracy). For example, *P. aeruginosa* which produces two siderophores pyoverdine **2** and pyochelin **3** (Figure 1),[35,36] will operate ENT secreted by other microorganisms through a specific TonB-dependent outer membrane transporter (TBDT), PfeA[37,38]. PfeA transports the ferric-ENT from the bacterial environment into the periplasm.[39] In the absence of PfeA, the TBDT PirA transports ferri-enterobactin complexes across the outer membrane in *P. aeruginosa* cells.[40] In the bacterial periplasm, the trilactone ring of the ferric-ENT is hydrolysed by the esterase PfeE into the Fe(III)-$(DHBS)_3$ complex.[16,41] Iron release from this complex requires probably a reduction step by a yet non-identified reductase. In vitro studies have shown that only the hydrolysis of enterobactin PfeE is not enough to dissociate iron from DHBS, but a reduction of iron is also needed.[16,41] This has been confirmed in E. coli where the dissociation of iron from enterobactin

involves a NADPH-dependent reductase, YdjH and the esterase Fes.[42-44] How iron is then transported further across the inner membrane into the bacteria cytoplasm remains unknown. The expression of PfeA and PfeE is induced by the presence of ferric ENT by a two-component regulation system PfeS/PfeR, where PfeS is the inner membrane sensor and PfeR the transcriptional activator (Figure 2).[45,46] The 3D structure of PfeA has been recently reported.[38] The protein harbors a TBDT fold with a barrel composed of 22 transmembrane ß strands obstructed by the N-terminal plug domain. The structure of PfeA loaded with ferric ENT has confirmed a biphasic recognition process, with a first binding site located in the extremity of the extracellular loops and a second deeper in the barrel located on the top of the plug domain.[38] The mechanism of translocation of ferri-siderophore complexes through TBDT is still unclear, but the current model suggests that the binding of ferric ENT to PfeA triggers the interaction between the PfeA "TonB box" and the inner membrane TonB complex, which provides the energy needed for the conformation change of the plug domain and the translocation of the ferric siderophore complex through the transporter. Such mechanism has been proposed for other TonB-dependent siderophore transporters.[47,48]

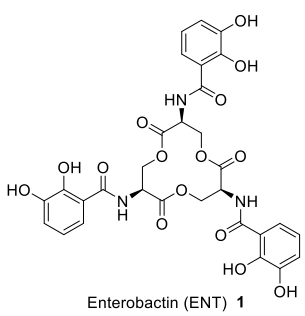

Enterobactin (ENT) **1**

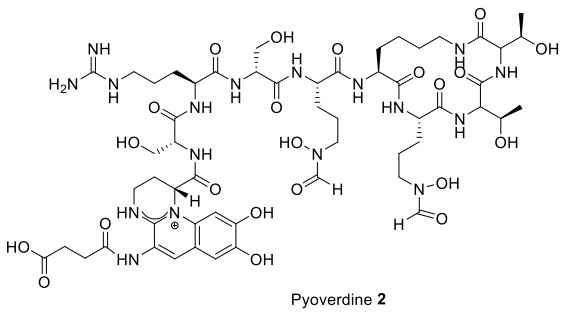

Pyoverdine **2**

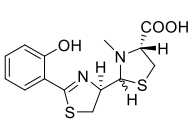

Pyochelin **3**

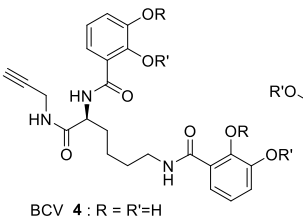

BCV **4** : R = R'=H
**6** : R-R' = $CPh_2$

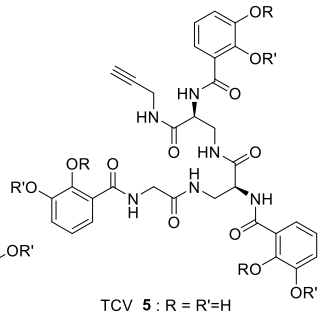

TCV **5** : R = R'=H
**7** : R-R' = $CPh_2$

**Figure 1.** Structures of siderophores enterobactin **1**, pyoverdine **2** and pyochelin **3** and of ENT inspired vectors BCV **4** and TCV **5** and their respective protected form **6** and **7**.

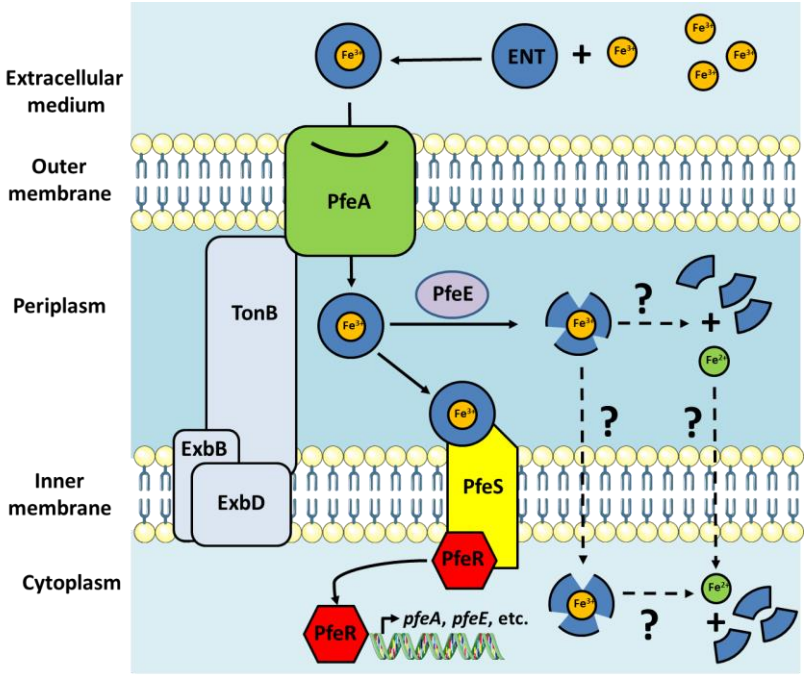


**Figure 2.** Enterobactin-dependent iron uptake pathway in *P. aeruginosa*. For more details see introduction.

Catechol vectors linked to oxazolidinones have shown activity against Gram-negative pathogens including *P. aeruginosa*.[40,50] An improved knowledge of the molecular mechanisms involved in the uptake of catechol type siderophore-antibiotic conjugates across the outer membrane, will enhance further development of next generation conjugates. We report here how PfeA interacts with different synthetic catechol siderophore-antibiotic conjugates, BCV **4** and TCV **5** (Bis- and Tris Catechol Vectors respectively)[51] coupled to linezolid (when unconjugated inactive against *P. aeruginosa*). We have shown previously,[39] that BCV **4** and TCV **5** both induce in *P. aeruginosa* cells the expression of the proteins of the ENT-dependent iron uptake pathway (PfeA and PfeE).[39,51] Here BCV- and TCV-conjugates proved to be invaluable molecular tools to investigate for the first time, the molecular basis of the interaction of siderophore-antibiotic conjugates with the outer membrane transporter.

# RESULTS AND DISCUSSION

## Bis- and Tris-catechol vectors interaction with PfeA transporter

We determined the structure of PfeA-$Fe^{3+}$-BCV and PfeA-$Fe^{3+}$-TCV to 2.7 and 2.6 Å resolution respectively. Both BCV **4** and TCV **5** bind to PfeA first binding site located in the extracellular loops (Figure 3a and 3b, Table S1, Figure S1 and S2 in ESI ) reported for ENT (Figure 3c to 3e, Figure S1 and S2 in ESI). Two of the catecholate rings occupy the same position as rings 2 and 3 of ENT. Key hydrogen bonds involved in the recognition between the catecholates of ENT and Gly325, Ser479, Arg480 and Gln482 are conserved. In the $Fe^{3+}$-TCV complex, the third catecholate has slightly shifted toward Arg480 (relative to ENT) to accommodate the propargyl arm. The stacking interaction of Arg480 with catecholate 2 is preserved. The two last atoms of the propargyl group were not clearly defined in the electron density map and were assumed to be disordered due to mobility. However, based on the well-ordered portion, the propargyl group points to the surface of the protein (Lys218 of L2) which is slightly displaced compared to the $Fe^{3+}$-ENT structure (Figure S1 in ESI). In the $Fe^{3+}$-BCV complex, the iron coordination sphere is completed by interaction with a molecule of ethylene glycol from buffer, (seen in PfeA-$Fe^{3+}$-azotochelin complex).[38] In the BCV ferric complex the propargyl group also points to Lys218.

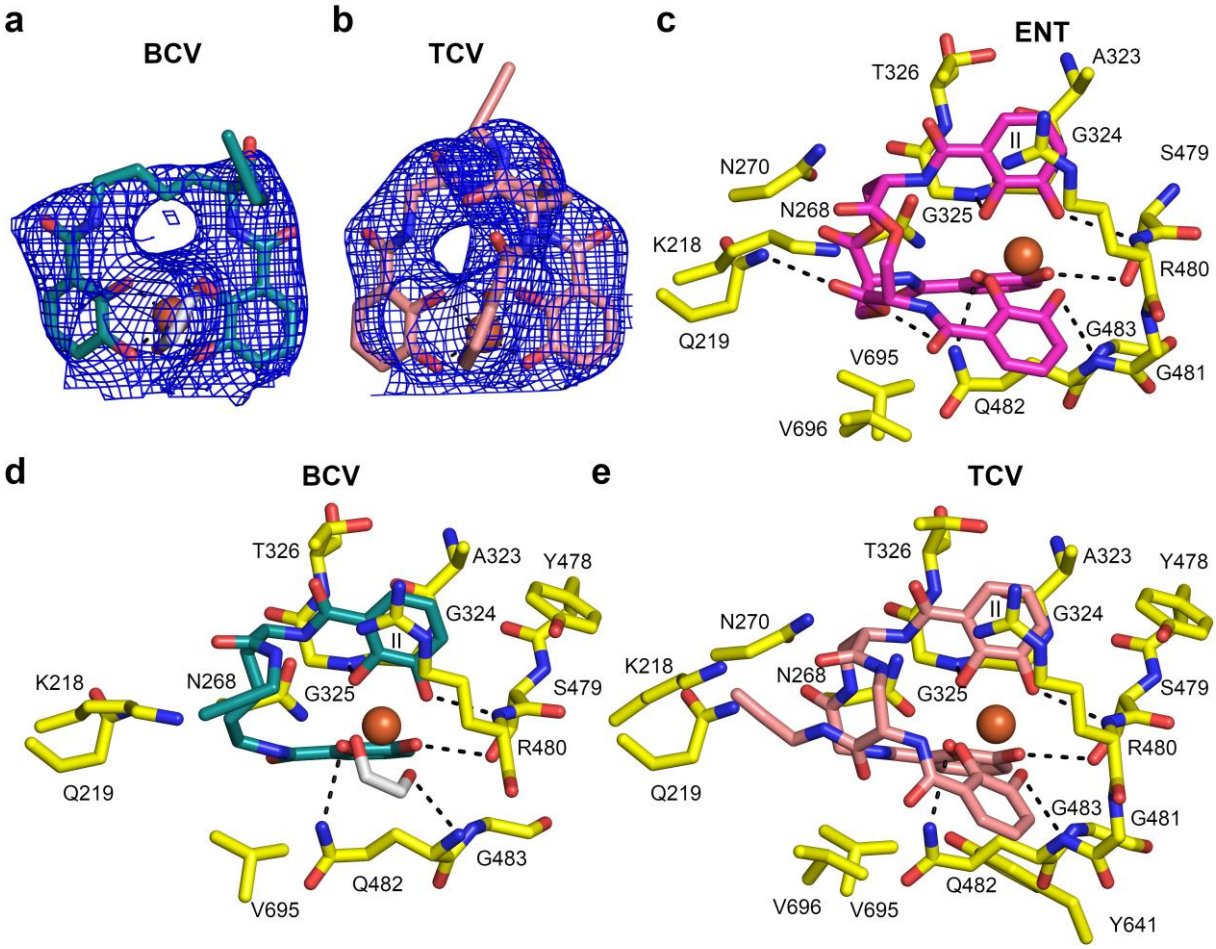


**Figure 3** : Structure of $Fe^{3+}$-BCV and $Fe^{3+}$-TCV in complex with PfeA. **a** and **b** Final $2F_O$-$F_C$ electron density map contoured at 1 σ level around $Fe^{3+}$-BCV and $Fe^{3+}$TCV respectively. Molecules are shown as sticks with carbon atoms coloured in deep teal (BCV) or salmon (TCV), nitrogen in dark blue and oxygen in red. The $Fe^{3+}$ is represented as an orange sphere. In PfeA-$Fe^{3+}$-BCV complex one ethylene glycol molecule (white sticks) completes the coordination shell of the iron. **c**, **d** and **e**, Comparison of the binding site of $Fe^{3+}$-ENT (pink, from 6Q5E)[38], $Fe^{3+}$-BCV and $Fe^{3+}$-TCV respectively. Residues within 4.0 Å of the siderophores are displayed and hydrogen bonds are shown as black broken lines.

Previous thermodynamic analysis (isothermal titration calorimetry ITC) of ENT titrated into PfeA showed a biphasic heat profile. Coupled to modelling studies this was interpreted as two cooperating binding sites, one high affinity site (~30 nM) and one lower affinity site (~190

μM), within PfeA.[38] Titration of both $Fe^{3+}$-BCV and of $Fe^{3+}$-TCV into PfeA by isothermal titration calorimetry (ITC) were best fitted to a single site binding model with a much-reduced enthalpy (-50-60 $kcal.mol^{-1}$) and lower affinity (19 μM for BCV and 21 μM for TCV) (Figure 4, Table S2, Figure S6 and S7 in ESI). ITC was repeated with PfeA double mutant (R480A-Q482A) and showed no binding for $Fe^{3+}$-TCV and considerably weaker binding for $Fe^{3+}$-BCV. These observations support the structural biology data that both catecholates bind to the first binding site of PfeA which governs siderophore recognition but do so with a significant reduction in affinity compared to the native ligand.

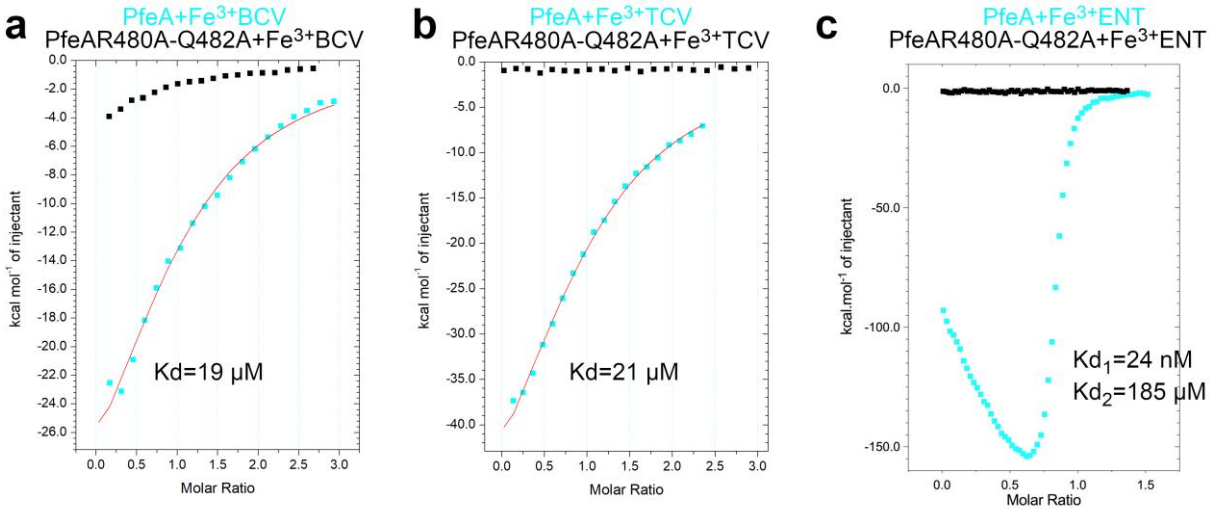


**Figure 4.** Comparison of the isothermal calorimetry titration of $Fe^{3+}$-BCV (**a**), $Fe^{3+}$-TCV (**b**) and $Fe^{3+}$-ENT(**c**) (shown for comparison but underlying data previously reported[38]) with PfeA (cyan) and mutants R480A-Q482A (black) show that $Fe^{3+}$-BCV and $Fe^{3+}$-TCV bind to PfeA specifically. The heats of dilution measured from injection of the ligands into the buffer were subtracted and TCV and BCV titration have been fitted with one-site interaction model instead of two binding sites.

## Signaling through the outer membrane promoted by Bis- and Tris-catechol vectors

Molecular dynamics simulations reported previously,[38] suggest that upon binding of $Fe^{3+}$-ENT to PfeA a signal transmits from extracellular loops to the N-terminal TonB box located in the periplasm.[38] This signal was suggested by means of Cα correlation, a method that allows for the detection of correlated concerted motion between distant sites in proteins,[52,53] which was performed in the same way as described in the method section of this work. The concerted motions between the binding site and the TonB box region were confirmed by a detailed analysis of crystallographic and simulation data where the chain of events leading to signal propagation was identified.[38] Here, Judged by Cα correlation in the MD structures, both BCV **4** (Figure 5D) and TCV **5** (Figure 5E) mimic the ENT (Figure 5C) signal transmission pathway, in that they showed strongly correlated pairs of residues separated by an average distance of at least 50Å connected via red lines (Figure 5C). In the empty transporter,[38] and double mutant there is no such correlation (Figure 5A and 5B respectively).

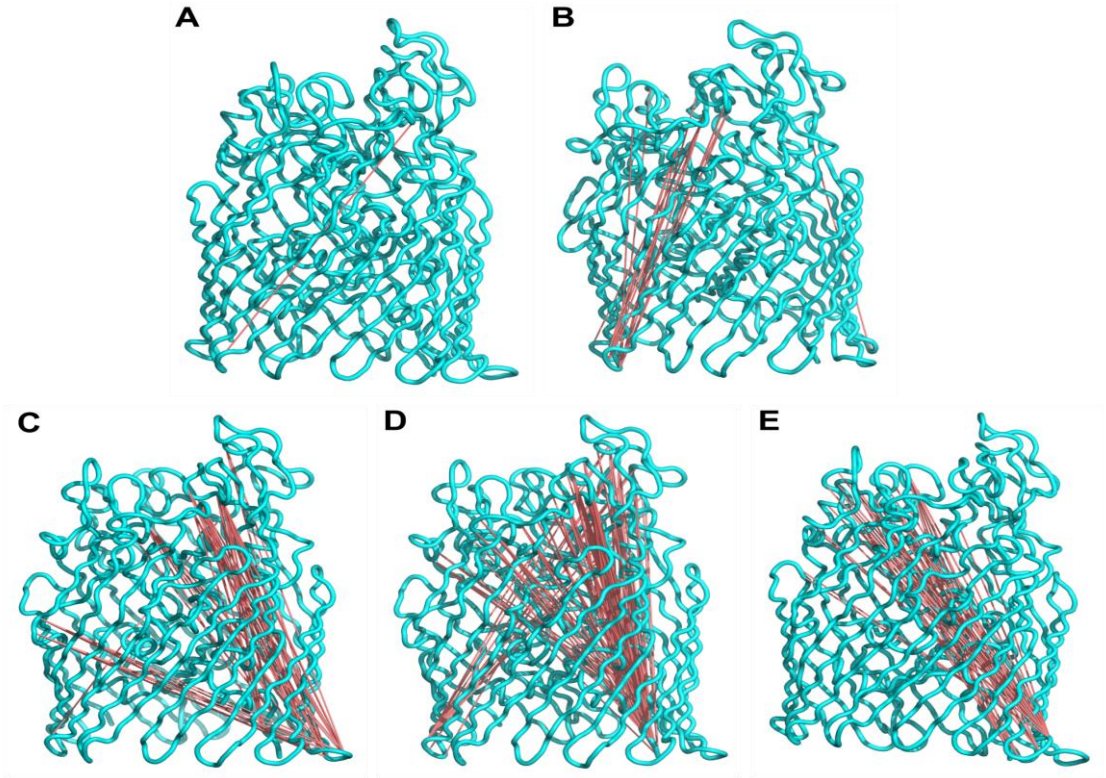

**Figure 5.** The Cα-correlation (>0.5) of distant residue pairs in (**A**) empty PfeA-apo. (**B**) PfeA R480A-Q482A. (**C**) PfeA-$Fe^{3+}$-ENT complex. (**D**) PfeA-$Fe^{3+}$-BCV **4** complex and (**E**) PfeA-$Fe^{3+}$-TCV **5** complex.

The correlation between the different structures can be visualised in full details plotting the Cα-correlation among all pairs of residues as a function of their separation (Figure S8, panel A-E in ESI) The long-distance signaling across different systems manifested in the rise of correlation above 50 Å, a distance comparable to the membrane thickness. Finally, the data are summarized in a form of cumulative histogram (Figure S8, panel F in ESI), which allows for the quantification of the effect counting the pairs with correlation larger than 0.4 and with the separation larger than 50 Å. We see a clear difference between systems with weak signaling (empty and double mutant PfeA), and systems with strong signaling (ferric ENT, ferric BCV **4**, and ferric TCV **5**). Interestingly, the strongest signal is detected in PfeA-$Fe^{3+}$-TCV **5** complex.

## Conjugation of oxazolidinones with bis- and tris-catechol vectors

Since both **4** and **5** were bound by PfeA and appeared to stimulate TonB signaling, we synthesized BCV- and TCV-oxazolidinone compounds. Protected BCV **6** and TCV **7** were reacted with oxazolidinone azides **8** and **9**,[54] using a copper(I)-catalyzed alkyne-azide cycloaddition (CuAAC).[55,56] Deprotection of the catechol functions of the resulting compounds in the presence of TFA led to the expected conjugates **10** to **13** isolated in respectively 70%, 83%, 52% and 36% yield over two combined synthetic steps. In conjugates **10** to **13** vectors and antibiotics are connected through a 1,2,3-triazole moiety (Scheme 1). The linkers were selected since the use of these conjugates as molecular tools requires a stability of the conjugation all along the uptake and signaling process. We also selected these structures to

investigate the effect of linkers of different size on the recognition of the conjugates and proteins involved in the uptake and signaling system.

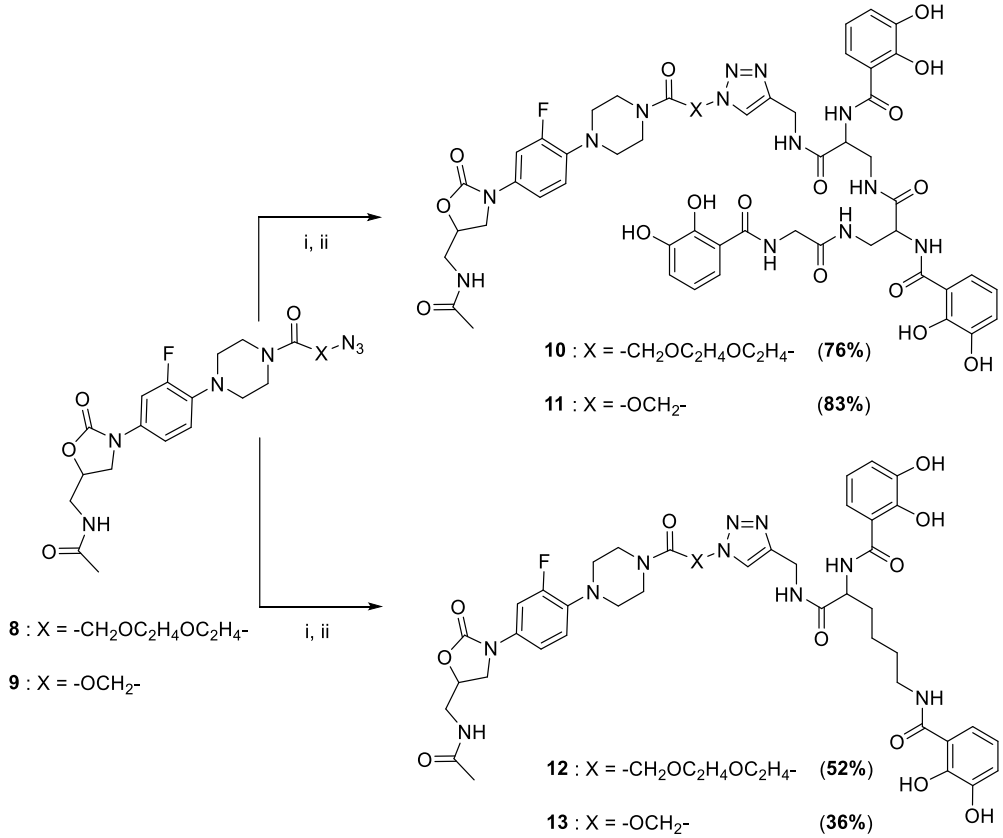


**Scheme 1.** Synthesis of TCV-oxazolidinone conjugates **10** and **11** and of BCV-oxazolidinone conjugates **12** and **13**. i. **6** or **7**, $CuSO_4$, sodium ascorbate, $THF/H_2O$, (((, 20°C. ii. $TFA/CH_2Cl_2$ 20%, TIPS, EtOH, 20°C.

## Antibacterial activity of oxazolidinones conjugates

The oxazolidinones antibiotic family of which linezolid serves as the example,[57] exert their effect by binding to the ribosomal 50S subunit. In *S. aureus* the conjugates **10** (MIC = 64 µM) and **11** (MIC =16 µM) retained some of the antibiotic activity of linezolid (MIC = 4 µM) showing that (1) the conjugates were transported into *S. aureus* cytoplasm and (2) oxazolidinone linked to the vector can still bind but with a lower activity than the oxazolidinone alone presumably due to the presence of the siderophore. Conjugates **10** to **13** had no significant

antibiotic activity on *P. aeruginosa* (MIC > 64 μM) suggesting these molecules are unable to interact with its target and/or unable to reach the ribosome in this pathogen (Table S3 in ESI).

## Interaction of catechol vectors-oxazolidinone conjugates with PfeA transporter

The X-ray structure between PfeA and the linezolid conjugates **10**, **11**, **12** and **13** showed the presence in the transporter first binding site of BCV and TCV moieties but no density was observed for the antibiotic conjugate (Figure S3 in ESI). The entire conjugate was observed in good electron density at the crystallographic interface between three molecules in the complex structure with **11** (Figure S4 in ESI). This finding, consistent with analytical data, suggests that the conjugate was not degraded but rather is disordered due to flexibility. Of course, the molecule bound at the crystal interface is a crystallization artefact and does not inform about transport. If the antibiotic is disordered, then the conjugate does not alter the recognition by PfeA (Figures S1, S2 and S5 in ESI). In the TCV conjugates **10** and **11**, a water molecule has been identified between two of the catecholates making hydrogen bonds with Arg480 and two amides of the TCV backbone (Figure S5e and S5f in ESI). A close inspection of TCV complex map suggests that a water molecule may occupy the same position in the structure but was not included as this was ambiguous. The titrations of $Fe^{3+}$-TCV **5** and $Fe^{3+}$-BCV **4** into PfeA by ITC show a much- weaker binding compared to $Fe^{3+}$-ENT. The addition of the linezolid connected by a short linker (TCV-L6 **11** and BCV-L6 **13**) has little additional effect (38 and 20 μM respectively) but a longer linker (TCV-L5 **10** and BCV-L5 **12**) does further reduce binding (100 and 37 μM) (Figure S6 and Table S2 in ESI). Molecular Dynamic (MD) simulations of PfeA in complex with ferric TCV-L6 **11** suggest that very fast after initial equilibration, TCV-L6 **11** moves into the second binding site (Figure S9 in ESI). This suggests that merged, the first and the second binding site could host molecules significantly larger than the ENT if the

initial interaction between the PfeA and the molecule induces a proper signal. By superimposing the poses of TCV-L6 on PfeA sampled with MD simulations (Figure 6), we see that the linezolid part fluctuates much more than the TCV part. Thus, it can be considered disordered, explaining the difficulties to catch it with X-ray diffraction.

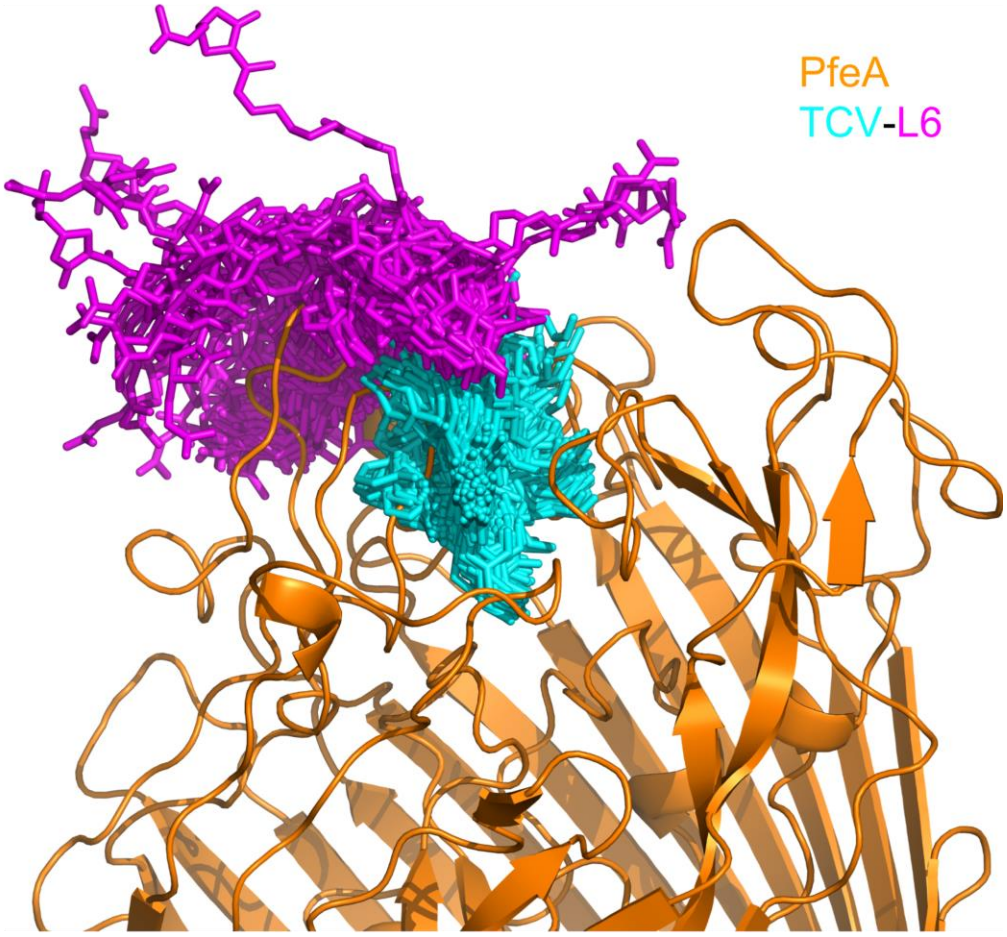


**Figure 6.** Dynamics of TCV-L6 **11** interaction with PfeA as extracted from MD simulations. The linezolid part of the molecule is shown in magenta, the TCV part is shown in cyan, and PfeA is given in orange. The linezolid part fluctuates much more than the TCV part and it can be considered disordered, explaining the difficulties to catch it with X-ray diffraction.

## The presence of the tris-catechol vector-oxazolidinone conjugates in the growth media of *P. aeruginosa* efficiently promotes the

## induction of the expression of PfeA and PfeE.

Crystallography and ITC indicate conjugates **10** to **13** bind their cognate outer membrane transporter PfeA. However, we were unable to carry out radioactive iron ($^{55}$Fe) uptake assays with sufficiently strong signal-to-noise ratio (SNR) to confirm transport (data not shown). The SNR arises from precipitation of iron loaded conjugates. Consequently, we investigated whether the conjugates **12** and **13** activate the same two-component system PfeS/PfeR as Fe-ENT. [45,46] Periplasmic Ferric ENT binds to PfeS sensor at the inner membrane activating the transcriptional regulator PfeR which upregulates the expression of the *pfeA* gene.[45,46] Induction of *pfeA* transcription in the presence of the conjugates implies that the compounds have crossed the bacterial OM since they can interact with PfeS only in the periplasm. Previous studies have shown that BCV **4** and TCV **5** vectors induce the transcription and expression of *pfeA* and *pfeE*.[16] *pfeA* and *pfeE* transcription are stronger with TCV than with BCV suggesting that either more TCV is transported than BCV or that PfeS binding site has a preference for the geometry of the Fe-TCV complex rather than that of the Fe-BCV complex. RT-qPCR analysis revealed that TCV conjugates **10** and **11** induced *pfeA* and *pfeE* transcription, indicating transport (Figure 7). Thus, the payload has not prevented transport into the periplasm or binding to the sensor. The induction of *pfeA* and *pfeE* transcription by TCV **5** and its conjugates **10** and **11** appeared stronger than the induction by ENT itself, a fact we attribute to the non-hydrolysable TCV **5** scaffold by PfeE.[16] Ferric complexes of TCV **5** and of TCV-oxazolidinone conjugates **10** and **11** accumulate in the bacterial periplasm leading to a sustained stimulation of the sensor but they do not cross the inner membrane to inhibit the ribosome. In contrast, although BCV **4** induces the expression of the main proteins of the ENT pathway it is weaker than the natural siderophore ENT and the vector TCV.[39] The BCV-oxazolidinone conjugates **12** and **13** show no induction of *pfeA* and *pfeE* and either are not transported or do not bind to PfeS. ENT, TCV, BCV nor their conjugates induced the expression of CirA and PirA, two TBDTs previously

described to be involved in the uptake of catechol siderophore and related conjugates (Figure 7).[40,58]

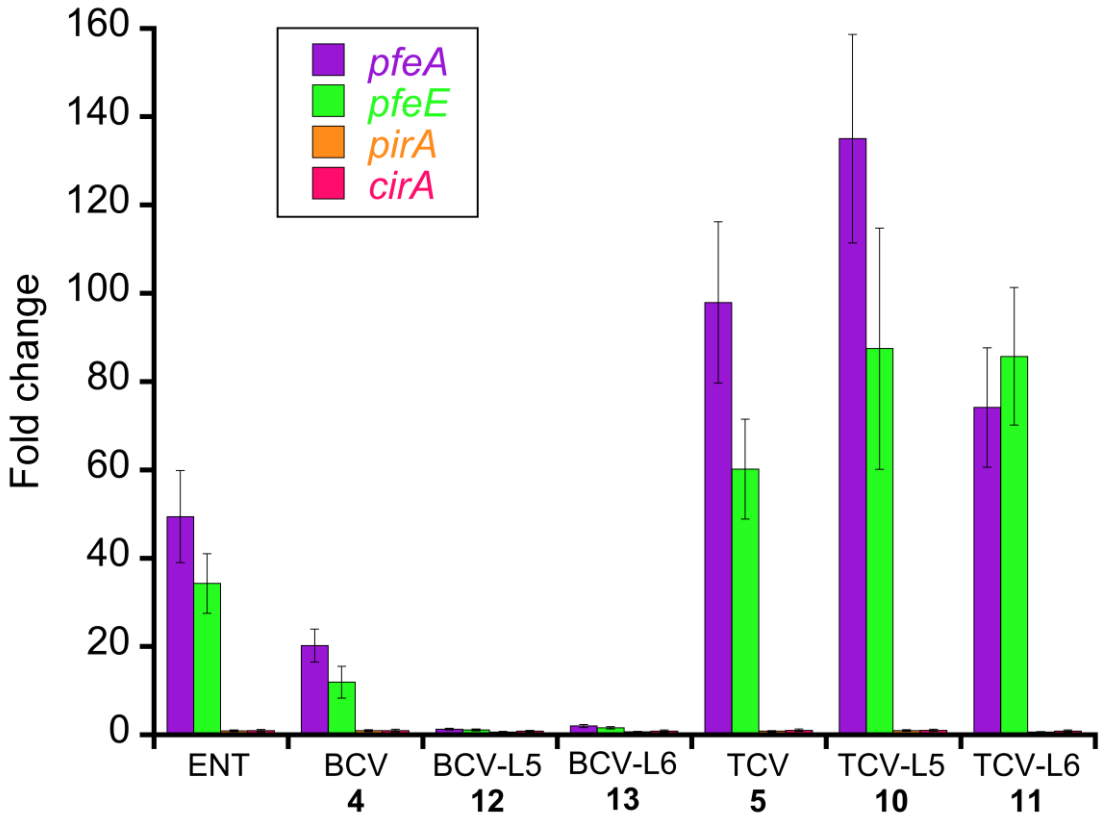


**Figure 7.** Analysis of changes in the transcription of the TBDT genes. RT-qPCR was performed on RNA from *P. aeruginosa* PAO1 cells grown in CAA medium, with and without supplementation with 10 µM ENT, BCV, TCV or conjugates **10** to **13**. The data are normalized relative to the reference gene *uvrD* and are representative of three independent experiments performed in triplicate (*n*=3). *pfeA* encodes for the TBDT of ENT, *pfeE* for the esterase involved in ENT hydrolyses, *pirA* and *cirA* for TBDT involved in iron acquisition by catechol siderophores.

## CONCLUSION

Catechol siderophores are used to access iron by many bacterial species even those unable to produce it. This predominance appears to be related to the extremely high affinity of catechol

siderophores for iron in comparison to other natural chelators, yielding a selective advantage in the competition for iron.[59] *P. aeruginosa* does not produce ENT but can use it as a siderophore by expressing PfeA a dedicated outer-membrane transporter and PfeE, a periplasmic esterase involved in the hydrolysis of the trilactone ring to facilitate iron release. These two proteins have their expression induced when *P. aeruginosa* is grown in the presence of ENT. Several research groups developed cargo based on the ENT or closely related molecule (Salmochelin) to efficiently deliver antibiotic and other xenobiotics into Gram-negative bacteria.[18,23,32,33] BCV **4** and TCV **5,** alternative ENT vectors used in the present study, are easy to prepare on gram scale and chemically stable compared to the trilactone core of the native siderophore. Moreover, the terminal alkyne of these vectors is a versatile chemical function to the conjugation of a broad range of linkers and payloads. We report here the synthesis of their conjugates **10** to **13** with an oxazolidinone antibiotic. These conjugates proved to be invaluable molecular tools to investigate, for the first time, the recognition process by the specific outer membrane transporter PfeA and the signaling induced across the transporter to get uptake of the compounds through the bacterial outer membrane. The BCV vector **4** was shown to mimic ENT in PfeA first binding site but the related conjugates failed to activate the two components system PfeS/PfeR located in the inner membrane and involved in the regulation of *pfeA* transcription. However, the TCV **5** as vector in Trojan horse strategies against *P. aeruginosa* showed more promise, both the ferric-vector and the ferric-oxazolidinone conjugates bind to PfeA at the same site as ferric-ENT and both result in the activation of the PfeS/PfeR system suggesting they are transported inside the bacterial periplasm. These are the properties required of a siderophore-based Trojan horse approach. Since the TCV derivatives are able to enter the bacterial periplasm, these conjugates are most suited to deliver antibiotics with periplasmic targets or whose linker specifically break down in the periplasm (thus allowing transport into the cytoplasm).

# ASSOCIATED CONTENT

The Supporting information is available free of charge at…

General considerations for structural biology, computational, chemical and microbiology experiments. Additional figures and tables. Experimental procedures for the synthesis of compound **10** to **13**. $^{1}H$, $^{19}F$ and $^{13}C$ NMR and LC/HRMS spectra of compounds **10** to **13**.

# AUTHOR INFORMATION

## Corresponding Authors

**Gaëtan L.A. Mislin -** CNRS/Université de Strasbourg UMR7242 Biotechnologie et Signalisation Cellulaire, Institut de Recherche de l'Ecole de Biotechnologie de Strasbourg (IREBS), 300 Boulevard Sébastien Brant, F-67412 Illkirch, Strasbourg, France. ORCID 0000-0002-5646-3392. Email : mislin@unistra.fr

## Authors

**Lucile Moynié -** The Rosalind Franklin Institute, Harwell Campus, Oxfordshire, UK OX11 0QS ORCID 0000-0002-4097-4331**.**

**Françoise Hoegy -** CNRS/Université de Strasbourg UMR7242 Biotechnologie et Signalisation Cellulaire, Institut de Recherche de l'Ecole de Biotechnologie de Strasbourg (IREBS), 300 Boulevard Sébastien Brant, F-67412 Illkirch, Strasbourg, France. ORCID 0000-0002-5440-5818.

**Stefan Milenkovic** - Dipartimento di Fisica, Università degli Studi di Cagliari, Cittadella Universitaria, 09042 Monserrato, Italy; IOM-CNR Unità di Cagliari, Cittadella Universitaria, 09042 Monserrato, Italy. ORCID 0000-0002-1327-3564.

**Mathilde Munier –** CNRS/Université de Strasbourg UMR7242 Biotechnologie et Signalisation Cellulaire, Institut de Recherche de l'Ecole de Biotechnologie de Strasbourg (IREBS), 300 Boulevard Sébastien Brant, F-67412 Illkirch, Strasbourg, France.

**Aurélie Paulen –** CNRS/Université de Strasbourg UMR7242 Biotechnologie et Signalisation Cellulaire, Institut de Recherche de l'Ecole de Biotechnologie de Strasbourg (IREBS), 300 Boulevard Sébastien Brant, F-67412 Illkirch, Strasbourg, France.

**Véronique Gasser –** CNRS/Université de Strasbourg UMR7242 Biotechnologie et Signalisation Cellulaire, Institut de Recherche de l'Ecole de Biotechnologie de Strasbourg (IREBS), 300 Boulevard Sébastien Brant, F-67412 Illkirch, Strasbourg, France. ORCID 0000-0002-0081-8000

**Aline L. Faucon –** CNRS/Université de Strasbourg UMR7242 Biotechnologie et Signalisation Cellulaire, Institut de Recherche de l'Ecole de Biotechnologie de Strasbourg (IREBS), 300 Boulevard Sébastien Brant, F-67412 Illkirch, Strasbourg, France. ORCID 0000-0002-7057-0485.

**Nicolas Zill –** CNRS/Université de Strasbourg UMR7242 Biotechnologie et Signalisation Cellulaire, Institut de Recherche de l'Ecole de Biotechnologie de Strasbourg (IREBS), 300 Boulevard Sébastien Brant, F-67412 Illkirch, Strasbourg, France.

**James H Naismith -** The Rosalind Franklin Institute, Harwell Campus, Oxfordshire, UK OX11 0QS ORCID 0000-0001-6744-5061.

**Matteo Ceccarelli –** Dipartimento di Fisica, Università degli Studi di Cagliari, Cittadella Universitaria, 09042 Monserrato, Italy; IOM-CNR Unità di Cagliari, Cittadella Universitaria, 09042 Monserrato, Italy. ORCID 0000-0003-4272-902X.

**Isabelle J. Schalk –** CNRS/Université de Strasbourg UMR7242 Biotechnologie et Signalisation Cellulaire, Institut de Recherche de l'Ecole de Biotechnologie de Strasbourg

(IREBS), 300 Boulevard Sébastien Brant, F-67412 Illkirch, Strasbourg, France. ORCID 0000-0002-8351-1679.

## Authors contributions

G.L.A.M, L.M., I.J.S, J.H.N. and M.C wrote the manuscript with inputs from the others. F.H., N.Z, A.P., M.M and A.L.F designed the target molecules, did the chemical experiments, purified, and characterized compounds **10** to **13** and their synthetic precursors. V.G. performed antibiotic assays and qRT-PCR experiments. I.J.S supervise microbiology experiments. S.M. designed, performed and analyzed molecular dynamic simulations. I.J.S, G.L.A.M., M.C. and J.H.N. find the grants.

## Competing Interest

Authors declare no competing interests

## ACKNOWLEDGMENTS

GLAM and IJS warmly thank *Vaincre la Mucoviscidose* and the *Association Grégory Lemarchal* (French associations against cystic fibrosis) for repeated financial support. GLAM acknowledges the *Agence Nationale pour la Recherche* (VECTRIUM project, ANR 19-CE18-0011-02) for financial support and for a PhD fellowship attributed to ALF. GLAM and IJS also acknowledge the Interdisciplinary Thematic Institute (ITI) InnoVec (Innovative Vectorization of Biomolecules, IdEx, ANR-10-IDEX-0002) and SFRI (ANR-20-SFRI-0012). AP acknowledges the *Ministère de l'Education Nationale, de l'Enseignement Supérieur et de la Recherche* (MENESR) for a PhD fellowship. Authors also acknowledge the *Centre National de la Recherche Scientifique* (CNRS) for general financial support. LM, SM, MM and NZ

acknowledge the Translocation consortium for their postdoctoral fellowships: the research leading to these results was conducted as part of the Translocation consortium (www.translocation.com) and benefitted from support from ND4BB ENABLE. All teams involved in the present work have received support from the Innovative Medicines Joint Undertaking under Grant Agreement n°115525 and n° 115583, resources which are composed of financial contributions from the European Union's seventh framework program (FP7/2007-2013) and EFPIA companies in kind contribution. Finally, authors acknowledge *Institut National de la Santé et de la Recherche Médicale* (INSERM) and AstraZeneca for granting the AnBRe project (IMMI_2014014). This work is supported by a Wellcome Trust Investigator (100209/Z/12/Z) award. MC and SM would like to thank Giuliano Malloci for providing the AMBER topology for the simulated molecules. MC thanks computer facilities at CINECA provided by the project "IscrB_PREDICT".

# REFERENCES

(1) Murphy, T.F. The Many Faces of *Pseudomonas aeruginosa* in Chronic Obstructive Pulmonary Disease. *Clin. Infect. Dis.* **2008**, *47*, 1534–1536.

(2) Folkesson, A.; Jelsbak, L.; Yang, L.; Johansen, H.K. Ciofu, O.; Høiby, N.; Molin, S. Adaptation of *Pseudomonas aeruginosa* to the cystic fibrosis airway: an evolutionary perspective. *Nat. Rev. Microbiol.* **2012**, *10*, 841–851.

(3) Schuster, M.; Norris, A. Community-acquired *Pseudomonas aeruginosa* pneumonia in patients with HIV infection. *AIDS* **1994**, *8*, 1437–1442.

(4) Church, D.; Elsayed, S.; Reid, O.; Winston, B.; Lindsay, R. Burn wound infections. *Clin. Microbiol. Rev.* **2006**, *19*, 403–434.

(5) Nikaido, H. Molecular basis of bacterial outer membrane permeability revisited. *Microbiol. Mol. Biol. Rev.* **2003**, *67*, 593-656.

(6) Raymond, K.N., Carrano, C.J. Coordination chemistry and microbial iron transport. Acc. Chem. Res. **1979**, *12*, 183–190.

(7) Braun, V.; Killmann, H. Bacterial solutions to the iron-supply problem. *Trends Biochem. Sci.* **1999**, *24*, 104–109.

(8) Cornelis, P.; Dingemans, J. *Pseudomonas aeruginosa* adapts its iron uptake strategies in function of the type of infections. *Front. Cell. Infect. Microbiol.* **2013**, *3*, 75.

(9) Hider, R.C.; Kong, X. Chemistry and biology of siderophores. *Nat. Prod. Rep.* **2010**, *27*, 637-657.

(10) Moynié, L. ; Serra, I. ; Scorciapino, M.A. ; Oueis , E.; Page, M.G.; Ceccarelli, M. ; Naismith, J.N. Preacinetobactin not acinetobactin is essential for iron uptake by the BauA transporter of the pathogen *Acinetobacter baumannii*. *elife* **2018**, *7*, e42270.

(11) Schalk, I.J.; Mislin, G.L.A.; Brillet, K. Structure, function and binding selectivity and stereoselectivity of siderophore-iron outer membrane transporters. *Curr. Top. Membr.* **2012**, *69*, 37-66.

(12) Klebba, P.E.; Newton, S.M.C.; Six, D.A.; Kumar, A.; Yang, T.; Nairn, B.L.; Munger, C.; Chakravorty, S. Iron Acquisition Systems of Gram-negative Bacterial Pathogens Define TonB-Dependent Pathways to Novel Antibiotics. *Chem. Rev.* **2021**, *121*, 9, 5193–5239.

(13) Noinaj, N.; Guillier, M.; Barnard, T.J.; Buchanan, S.K. TonB-dependent transporters: regulation, structure, and function. *Annu. Rev. Microbiol.* **2010**, *64*, 43-60.

(14) Celia, H.; Noinaj, N.; Zakharov, S.D.; Bordignon, E.; Botos, I.; Santamaria, M.; Barnard, T.J.; Cramer, W.A.; Lloubes, R.; Buchanan, S.K. Structural insight into the role of the Ton complex in energy transduction. *Nature* **2016**, **538**, 60-65.

(15) Schalk, I.J.; Guillon, L. Fate of ferrisiderophores after import across bacterial outer membranes: different iron release strategies are observed in the cytoplasm or periplasm depending on the siderophore pathways. *Amino Acids* **2013**, 44,1267-1277.

(16) Perraud, Q.; Moynié, L.; Gasser, V.; Munier, M.; Godet, J.; Hoegy, F.; Mély, Y.; Mislin, G.L.A.; Naismith, J.H.; Schalk, I.J. A Key Role for the Periplasmic PfeE Esterase in Iron Acquisition via the Siderophore Enterobactin in *Pseudomonas aeruginosa*. *ACS Chem. Biol.* **2018**, *13*, 2603-2614.

(17) Mislin, G.L.A.; Schalk, I.J. Siderophore-dependent iron uptake systems as gates for antibiotic Trojan horse strategies against *Pseudomonas aeruginosa*. *Metallomics* **2014**, *6*, 408-420.

(18) Neumann, W. ; Sassone-Corsi, M. ; Raffatellu, M. ; Nolan, E.M. Esterase-catalyzed siderophore hydrolysis activates an enterobactin-ciprofloxacin conjugate and confers targeted antibacterial activity. *J. Am. Chem. Soc.* **2018**, *140*, 5193–5201.

(19) Fardeau, S.; Dassonville-Klimpt, A.; Audic, N. ; Sasaki, A.; Pillon, M.; Baudrin, E.; Mullié, C. ; Sonnet, P. Synthesis and antibacterial activity of catecholate-ciprofloxacin conjugates. *Bioorg. Med. Chem.* **2014**, *22*, 4049-4060.

(20) Ji, C.; Miller, P.A.; Miller, M.J. Iron Transport-Mediated Drug Delivery: Practical Syntheses and In Vitro Antibacterial Studies of Tris-Catecholate Siderophore–Aminopenicillin Conjugates Reveals Selectively Potent Antipseudomonal Activity. *J. Am. Chem. Soc.* **2012**, *134*, 9898-9901.

(21) Möllmann, U.; Heinisch, L.; Bauernfeind, A.; Köhler, T.; Ankel-Fuchs, D. Siderophores as drug delivery agents: application of the "Trojan Horse" strategy. *Biometals* **2009**, 22, 615-624.

(22) Milner, S.J.; Seve, A.; Snelling, A.M.; Thomas, G.H.; Kerr, K.G.; Routledge, A.; Duhme-Klair, A.-K.. Staphyloferrin A as siderophore-component in fluoroquinolone-based Trojan horse antibiotics. *Org. Biomol. Chem.* **2013**, *11*, 3461-3468.

(23) Sanderson, T.J.; Black, C.M.; Southwell, J.W.; Wilde, E.J.; Pandey, A.; Herman, R.; Thomas, G.H.; Boros, E.; Duhme-Klair, A.-K.; Routledge, A. A Salmochelin S4-Inspired Ciprofloxacin Trojan Horse Conjugate. *ACS Infect. Dis.* **2020**, *6*, 2532-2541.

(24) Scorciapino, M.A.; Malloci, G.; Serra, I.; Milenkovic, S.; Moynié , L.; Naismith, J.H.; Desarbre, E.; Page, M.G.; Ceccarelli, M. Complexes formed by the siderophore-based monosulfactam antibiotic BAL30072 and their interaction with the outer membrane receptor PiuA of *P. aeruginosa*. *Biometals* **2019**, 32, 155-170.

(25) de Carvalho, C.C.C.R.; Fernandes,P. Siderophores as "Trojan Horses": tackling multidrug resistance? *Front Microbiol.* **2014**, *5*, 290

(26) Kong, H.; Cheng, W.; Wei, H.; Yuan, Y.; Yang, Z.; Zhang, X. An overview of recent progress in siderophore-antibiotic conjugates. *Eur. J. Med. Chem.* **2019**, *182*, 111615.

(27) Negash, K.H.; Norris, J.K.S.; Hodgkinson, J.T. Siderophore-Antibiotic Conjugate Design: New Drugs for Bad Bugs? *Molecules* **2019**, 24, 3314.

(28) Lin, Y.M.; Ghosh, M.; Miller, P.A.; Möllmann, U.; Miller, M.J. Synthetic sideromycins (skepticism and optimism): selective generation of either broad or narrow spectrum Gram-negative antibiotics. *Biometals* **2019**, 32, 425-451.

(29) Górska,A.; Sloderbach, A.; Marszałł, M.P. Siderophore-drug complexes: potential medicinal applications of the 'Trojan horse' strategy. *Trends Pharmacol. Sci.* **2014**, 35, 442-449.

(30) Liu, R.; Miller, P.A.; Miller, M.J. Conjugation of Aztreonam, a Synthetic Monocyclic β-Lactam Antibiotic, to a Siderophore Mimetic Significantly Expands Activity Against Gram-Negative Bacteria. *ACS Infect Dis* **2021**, *7*, 2979-2986.

(31) Pinkert, L.; Lai, Y.H.; Peukert, C.; Hotop, S.K.; Karge, B.; Schulze, L.M.; Grunenberg, J.; Brönstrup, M. Antibiotic Conjugates with an Artificial MECAM-Based Siderophore Are Potent

Agents against Gram-Positive and Gram-Negative Bacterial Pathogens. *J. Med. Chem.* **2021**, *64*, 15440-15460.

(32) Zscherp, R.; Coetzee, J.; Vornweg, J.; Grunenberg, J.; Herrmann, J.; Müller, R.; Klahn, P. Biomimetic enterobactin analogue mediates iron-uptake and cargo transport into *E. coli* and *P. aeruginosa*. *Chem Sci.* **2021**, 12, 10179-10190.

(33) Advances in the synthesis of enterobactin, artificial analogues and enterobactin-derived antimicrobial drug conjugates and imaging tools for infection diagnosis, P. Klahn, R. Zscherp, C. C. Jimidar, *Synthesis* **2022**, *in press.* DOI: 10.1055/a-1783-0751.

(34) Raymond; K.N.; Dertz, E.A.; Kim, S.S. Enterobactin: an archetype for microbial iron transport. *Proc. Natl. Acad. Sci. USA* **2003**,*100*, 3584-3588.

(35) Cox, C.D.; Rinehart, K.L. Jr; Moore, M.L.; Cook, J.C. Jr. Pyochelin: novel structure of an iron-chelating growth promoter for *Pseudomonas aeruginosa*. *Proc. Natl. Acad. Sci. USA.* **1981**,*78*, 4256-4260.

(36) Abdallah, M.A.; Pfestorf, M.; Döring, G. *Pseudomonas aeruginosa* pyoverdin: structure and function. *Antibiot. Chemother.* **1989**, *42*, 8-14.

(37) Dean, C.R.; Poole, K. Expression of the ferric enterobactin receptor (PfeA) of *Pseudomonas aeruginosa*: involvement of a two-component regulatory system. *Mol. Microbiol.* **1993**, *8*, 1095–1103.

(38) Moynié, L.; Milenkovic, S.; Mislin, G.L.A.; Gasser, V.; Malloci, G.; Baco, E.; McCaughan, R.P.; Page, M.G.P.; Schalk, I.J.; Ceccarelli, M.; Naismith, J.H. The complex of ferric-enterobactin with its transporter from *Pseudomonas aeruginosa* suggests a two-site model. *Nat. Commun.* **2019**, *10*, 3673.

(39) Gasser, V.; Baco, E.; Cunrath, O.; Saint-August, P.; Perraud, Q.; Zill, N.; Schleberger, C.; Schmidt, A.; Paulen, A.; Bumann, D.; Mislin, G.L.A.; Schalk, I.J. Catechol siderophores repress the pyochelin pathway and activate the enterobactin pathway in *Pseudomonas*

*aeruginosa*: an opportunity for siderophore-antibiotic conjugates development. *Environ. Microbiol.* **2016**, *18*, 819-832.

(40) Ghysels, B.; Ochsner, U.; Mollman, U.; Heinisch, L.; Vasil, M.; Cornelis, P.; Matthijs, S. The *Pseudomonas aeruginosa* pirA Gene Encodes a Second Receptor for Ferrienterobactin and Synthetic Catecholate Analogues. *FEMS Microbiol. Lett.* **2005**, *246*, 167–174.

(41) Gasser, V., Kuhn, L.; Hubert, T.; Aussel, L.; Hammann, P.; Schalk, I.J. The Esterase PfeE, the Achilles' Heel in the Battle for Iron between *Pseudomonas aeruginosa* and *Escherichia coli*. *Int. J. Mol. Sci.* **2021**, 22, 2814.

(42) Brickman, T.J.; McIntosh, M.A. Overexpression and Purification of Ferric Enterobactin Esterase from *Escherichia coli*. Demonstration of Enzymatic Hydrolysis of Enterobactin and Its Iron Complex. *J. Biol. Chem.* **1992**, *267*, 12350–12355.

(43) Lin, H.; Fischbach, M.A.; Liu, D.R.; Walsh, C.T. In Vitro Characterization of Salmochelin and Enterobactin Trilactone Hydrolases IroD, IroE, and Fes. J. Am. Chem. Soc. **2005**, *127*, 11075–11084.

(44) Miethke, M.; Hou, J.; Marahiel, M.A. The Siderophore-Interacting Protein YqjH Acts as a Ferric Reductase in Different Iron Assimilation Pathways of *Escherichia coli*. *Biochemistry* **2011**, *50*, 10951–10964.

(45) Dean, C.R.; Neshat, S.; Poole, K. PfeR, an enterobactin-responsive activator of ferric enterobactin receptor gene expression in *Pseudomonas aeruginosa*. *J. Bacteriol.* **1996**, *178*, 5361-5369.

(46) Dean, C.R.; Poole, K. Expression of the ferric enterobactin receptor (PfeA) of *Pseudomonas aeruginosa*: involvement of a two-component regulatory system. *Mol. Microbiol.* **1993**, *8*,1095-1103.

(47) Josts, I; Veith, K.; Tidow, H. Ternary structure of the outer membrane transporter FoxA with resolved signalling domain provides insights into TonB-mediated siderophore uptake. *eLife* **2019**, *8*, e48528.

(49) Grinter, R.; Lithgow, T. The structure of the bacterial iron-catecholate transporter Fiu suggests that it imports substrates via a two-step mechanism. *J. Biol. Chem.* **2019**, *294*, 19523-19534.

(49) Paulen, A.; Gasser, V.; Hoegy, F.; Perraud, Q.; Pesset, B.; Schalk, I.J.; Mislin, G.L.A. Synthesis and antibiotic activity of oxazolidinone-catechol conjugates against *Pseudomonas aeruginosa*. *Org. Biomol. Chem.* **2015**, *13*,11567-151179.

(50) Liu, R.; Miller, P.A.; Vakulenko, S.B.; Stewart, N.K.; Boggess, W.C.; Miller, M.J .A Synthetic Dual Drug Sideromycin Induces Gram-Negative Bacteria To Commit Suicide with a Gram-Positive Antibiotic. *J. Med. Chem.* **2018**, *61*, 3845-3854.

(51) Baco, E.; Hoegy, F.; Schalk, I.J.; Mislin, G.L.A. Diphenyl-benzo[1,3]dioxole-4-carboxylic acid pentafluorophenyl ester: a convenient catechol precursor in the synthesis of siderophore vectors suitable for antibiotic Trojan horse strategies. *Org. Biomol. Chem.* **2014**, *12*, 749-57.

(52) Ichiye, T ; Karplus, M. *Proteins* **1991**, *3*, 205-217.

(53) Lange, O. F.; Grubmüller, H. Generalized correlation for biomolecular dynamics. *Proteins* **2006**, *62*, 1053–1061.

(54) Paulen, A.; Hoegy, F.; Roche, B.; Schalk, I.J.; Mislin, G.L.A. Synthesis of conjugates between oxazolidinone antibiotics and a pyochelin analogue. *Bioorg. Med. Chem. Lett.* **2017**, *27*, 4867-4870.

(55) Rostovtsev, V.V.; Green, L.G.; Fokin, V.V.; Sharpless, K.B. A Stepwise Huisgen Cycloaddition Process: Copper(I)-Catalyzed Regioselective Ligation of Azides and Terminal Alkynes. *Angew. Chem. Int. Ed. Engl.*, **2002**, *41*, 2596-2599.

(56) Tornøe, C.W.; Christensen, C.; Meldal, M. Peptidotriazoles on Solid Phase: [1,2,3]-Triazoles by Regiospecific Copper(I)-Catalyzed 1,3-Dipolar Cycloadditions of Terminal Alkynes to Azides. *J. Org. Chem.* **2002**, *67*, 3057–3064.

(57) Bozdogan, B.; Appelbaum, P.C. Oxazolidinones: activity, mode of action, and mechanism of resistance. *Int. J. Antimicrob. Agents* **2004**, *23*, 113-119.

(58) Luscher, A.; Moynié, L.; Saint-August, P.; Bumann, D.; Mazza, L.; Pletzer, D.; Naismith, J.H.; Köhler, T. TonB-Dependent Receptor Repertoire of *Pseudomonas aeruginosa* for Uptake of Siderophore-Drug Conjugates. *Antimicrob. Agents Chemother.* **2018**, *62*, e00097-18

(59) Perraud, Q.; Cantero, P.; Roche, B.; Gasser, V.; Normant, V.P.; Kuhn, L.; Hammann, P.; Mislin, G.L.A.; Ehret-Sabatier, L; Schalk, I.J. Phenotypic adaption of *Pseudomonas aeruginosa* by hacking siderophores produced by other microorganisms. *Mol. Cell. Proteomics* **2020**, *19*, 589-607.